


Rankine cycle power augmentation: a comparative case study on the introduction of ORC or absorption chiller

Vitor R. Seifert¹  · Yuri M. Barbosa¹ · Júlio A. M. da Silva² · Ednildo A. Torres³

Received: 28 March 2017 / Accepted: 28 August 2017 / Published online: 12 September 2017
© The Brazilian Society of Mechanical Sciences and Engineering 2017

Abstract The search for more efficient processes to save resources and avoid further environmental damages is mandatory in the current society. Increase in power and efficiency of already existing power plants play important role in the transition to more efficient cycles. This work compares two different thermal arrangements that can be fitted in already existing Rankine cycle power plants to improve their power and efficiency. These arrangements are possible when fuel sulfur concentration is reduced to meet stricter SO_x emission legislation. The first thermal arrangement is composed of an absorption chiller and a chilled water storage tank designed to make use of the energy remaining in boiler exhaust gases. Thermal accumulation enables the use of an absorption chiller to produce chilled water during the period of 24 h. This chilled water is used in the condenser during peak hours to increase power output and the efficiency of the plant. The second

option is fitting an optimized organic Rankine cycle (ORC) also powered by the exhaust gases from the boiler. Results show that fitting an ORC using *n*-butane as a working fluid represents a gain of 409.3 kW on net power and 0.42% on efficiency against 55.92 kW and 0.07% obtained using the absorption chiller. Therefore, from a thermodynamic point of view, it is more interesting to use optimized ORCs than absorption chillers for existing power plants operating under the operational conditions evaluated.

Keywords Repowering · Rankine cycle · Power plant · Absorption chiller · ORC

1 Introduction

The search for renewable energy sources and increasing energy efficiency in power generation has been a common concern in recent years. In addition, there is a concern over emissions of greenhouse gases such as CO₂ from fossil fuel combustion. Some studies aim at increasing efficiency and consequently reducing the usage of fossil fuel to generate electricity. Most thermal power plants are based on Rankine cycles, gas turbines (Brayton cycle), alternative engines (otto/diesel) or a combination of these technologies. The efficiency of these systems may be increased using absorption chillers or organic Rankine cycles (ORC) powered by the exergy remaining in the heat wasted by these power plants.

The use of cooling equipment to enhance the power generation is extensively present in the literature. The performance of gas turbines for example is dependent on ambient temperature [15]. The most common application for cooling equipment to enhance power production is reducing the temperature of gas turbine inlet air to increase

Technical Editor: Jose A. dos Reis Parise.

✉ Vitor R. Seifert
vitor.seifert@ufba.br

Yuri M. Barbosa
yuri_mbarbos@hotmail.com

Júlio A. M. da Silva
julio.silva@ufba.br

Ednildo A. Torres
ednildotorres@gmail.com

¹ Industrial Engineering Program, Federal University of Bahia, Rua Aristides Novis 2, Federação, Salvador, Bahia CEP 40210-630, Brazil

² Department of Mechanical Engineering, Federal University of Bahia, Salvador, Bahia, Brazil

³ Department of Chemical Engineering, Federal University of Bahia, Salvador, Bahia, Brazil

the air mass flow rate through the equipment and also to reduce compressor power consumption [6]. Shirazi et al. [22] presented a mathematical model for an ice thermal energy storage (ITES) system applied to cool the gas turbine inlet air. It was concluded that using ITES, an improvement of 11.63% in power output and 3.59% in the exergy efficiency can be achieved. The efficiency of power plants based on Rankine cycle depends on the condensation temperature. A reduction in this temperature results in reduction of condensation pressure, which means more power output during the expansion in the steam turbine and consequently greater plant efficiency. A particular plant may have an increase of around 10% in power generation when the condenser pressure is changed from 0.087 to 0.033 bar [2]. Muñoz et al. [18] analyzed the performance of a Rankine cycle in which the energy from boiler exhausting gases was used to feed an absorption chiller to chill the condenser cooling water. The conclusion was that the energy of exhausting gases was not enough to significantly reduce the temperature of cooling water due to the high mass flow rate of this stream. In the present work, the use of a cold water tank to store the water cooled by the absorption chiller is proposed. This water will be used during hours of peak consumption to increase the power produced by the power plant.

Recently, ORCs have been studied due to their ability to use low-grade heat sources such as waste heat from industry, geothermal energy and solar energy to produce electricity [4]. ORCs are more interesting than conventional Rankine cycles, which use water/steam as a working fluid, due to their physical properties more adequate to deal with low temperature heat sources. Some of the important properties are the positive inclination of vapor saturation line and proper condensation and evaporation pressure under the temperatures of the environment and the heat sources, respectively. The use of organic fluids also results in more compact system and reduces the costs of implementation and maintenance of the system [20]. Song et al. [26] analyzed an ORC to recover waste heat from marine diesel engines using jacket cooling water and the exhaust gases to obtain maximum power output. The cycle that used the jacket cooling water to pre-heat the working fluid and the exhaust gases to evaporate it resulted in a gain of 99.7 kW in power generation with low implementation costs. Galindo et al. [11] analyzed thermodynamically and experimentally an ORC using waste heat from a gasoline engine. Other authors such as Shu et al. [23] and Battista et al. [3] studied the effects of the operational characteristics on the performance of ORCs attached to combustion engines. The first concluded that azeotropic mixtures of organic fluids result in lower efficiencies than most pure organic fluids, while zeotropic mixtures, in certain proportions, result in higher efficiency when compared to the

same pure organic fluids. The second concluded that the installation of an ORC coupled to a conventional gasoline engine with turbo-compressor can increase the mechanical efficiency of the system in up to 3.7%.

Chacartegui et al. [7] analyzed the applicability of ORC in using the exhaust gases from regenerative gas turbines. This configuration compared to conventional gas turbines results in exhaust gases at lower temperatures which can be used as heat source for the ORC. The system optimization was conducted based on gas turbine inlet temperature and resulted in a gain of efficiency superior to those from the combined cycles presented in the literature. Clemente et al.'s [9] study was focused on the application of an ORC to use exhaust gases from small scale gas turbines (100 kWe). Comparing the options for the ORC expanders, the author concluded that single stage turbines are more advantageous than positive displacement expanders because they can be connected to the gas turbine shaft and produce higher gains in efficiency to the whole system. For this application, micro-turbines, refrigerant fluids are more suitable because they allow the use of compact equipments. Camporeale et al. [5] analyzed thermodynamically and technical economically an ORC using waste heat from a non-regenerative gas turbine powered by biomass. The absence of a regenerator results in higher temperature of the exhaust gases. It was concluded that superheating on subcritical ORCs causes efficiency losses. Therefore, it is preferable to use cycles with evaporation close to the saturation line. The same issue was observed for supercritical cycles. In this case, the parameters should be kept next to the critical point. For this specific application, the most suitable fluid is the toluene due to its high heat recovery rate. Chacartegui et al. [8] studied the application of an ORC to use exhaust gases from a humid air turbine for distributed micro-generation. Results show a gain of 25% in power generated which corresponds to an increase of 11% in the efficiency when compared to an isolated gas turbine. The economical analysis showed a reduction of 15% on the cost of electricity which indicates that this technology is highly competitive for the proposed application. Demierre et al. [10] designed a prototype of a thermally driven heat pump, which consisted in two ORC coupled, one generating shaft power to rotate a compressor of a reversed ORC which worked as the heat pump. The upper ORC consisted in a supercritical ORC which used R134a as the working fluid. The hot heat source used is the combustion gases from stoichiometric combustion of methane. The cold heat source is the brine from a geothermal probe. The results of the experiment are compared to the simulations and resulted on a difference of less than 3% between the predicted overall heat transfer and the measurements.

In this work, the ORC makes use of the opportunity created when the fuel used in a boiler is replaced by a fuel with lower sulfur concentration, therefore, the energy remaining in exhausting gases can be further used without reaching the acid condensation point. An optimization procedure is performed to find the configuration which provides maximum power output for each tested fluid. The result of the best ORC scheme is compared to the result from using energy storage and an absorption chiller to chill condenser cooling water.

2 System modeling

For this work, a typical power plant based on Rankine cycle is used. The following sub topics present some simplifying assumptions, the characteristics of the power plant and the proposed changes to increase both power generation and plant efficiency.

2.1 Simplifying assumptions

1. Changes in potential and kinetic energies are considered negligible.
2. All components operate under steady state condition except for the water tanks.
3. The pressure drop in pipelines is disregarded.
4. Environment temperature and humidity remains constant along the analysis.

2.2 Studied Rankine cycle-based power plant

This analysis is carried out considering the power plant shown in Fig. 1.

The boiler produces 27.78 kg/s (100 ton/h) of steam at 485 °C and 9100 kPa. These data follow those from the conventional boilers installed in the biggest Brazilian

refinery [24, 25]. Exhaust gases leave at 175.6 °C. Saturated steam enters into the condenser at 45 °C. The water exits the cooling tower at 30 °C and returns from condenser at 40 °C. The temperature and pressure of the subcooled liquid leaving the deaerator are, respectively, 133 °C and 300 kPa. All pumps have isentropic efficiency of 80%. The steam turbine has isentropic efficiency of 85% and the boiler has thermal efficiency of 92%. Tables 1 and 2 show, respectively, the properties of each stream of the plant and the global information.

2.3 Exhausting gas acid dew point

According to Ganapathy [12], if the temperature of the exhausted gases reaches the acid dew point temperature, corrosion problems may occur. It is a general trend, nowadays, the replacement of sulfur rich fuels by fuels with lower concentration of this element to avoid excessive SO_x emissions. The most well-known example in Brazil is the gradual replacement of S1800 diesel by S10 diesel during the last decades [1, 19]. This kind replacement also allows further use of exhausting gas energy because the dew point temperature will be lowered as the sulfur concentration decreases. Table 3 shows some commonly used fuel, their composition and dew point. Fuel oil 1A was selected due to its lower amount of sulfur as the substitute to the originally used fuel, a refinery fuel oil (not commercially available), which allows 175.6 °C as exhausting temperature.

2.4 First proposal: absorption chiller

In this proposal an absorption chiller is coupled to the boiler of the power plant to make use of boiler exhaust gases as heat source. During the operation of the plant, the chiller cools water and directs it into the cold water storage tank. At peak electricity consumption hours, the stored cold water is drained into the condenser, replacing the cooling water from cooling tower. The cold water stored reduces

Fig. 1 Studied power plant

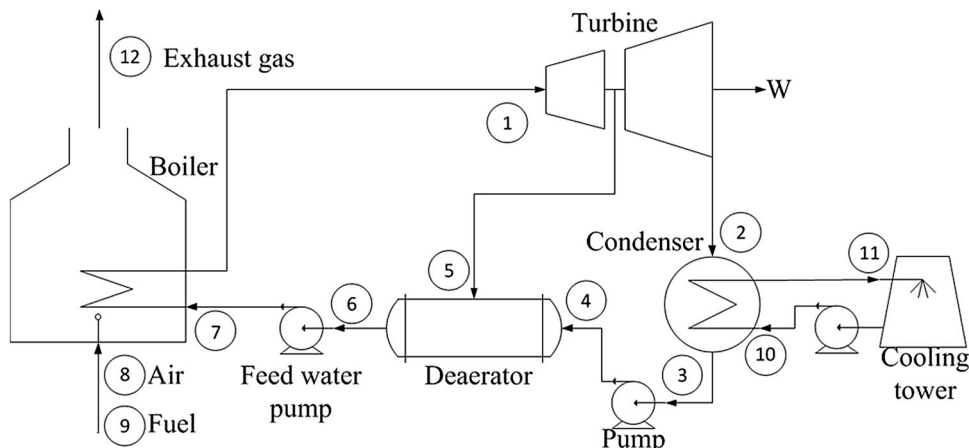


Table 1 Studied power plant thermodynamic properties

Stream	Mass flow (kg/s)	Pressure (kPa)	Temperature (°C)	Quality	Enthalpy (kJ/kg)	Entropy (kJ/kg K)
1	27.78	9100.0	485.00	–	3347.86	6.6038
2	23.68	9.6	45.00	0.83	2175.98	6.8858
3	23.68	9.6	45.00	0.00	188.44	0.6388
4	23.68	300.0	45.05	–	188.85	0.6392
5	4.10	300.0	133.53	0.98	2684.31	6.8918
6	27.78	300.0	132.53	–	557.19	1.6614
7	27.78	9100.0	133.93	–	569.05	1.6674
8	33.97	101.3	25.00	–	–	–
9	2.08	101.3	25.00	–	–	–
10	1126.93	229.5	31.00	–	143.86	0.4306
11	1126.93	200.0	40.00	–	185.17	0.5646
12	35.73	101.3	175.61	–	187.77	0.7600

Table 2 Global information of the studied power plant

Global data	Value	Unit
$W_{\text{tot_gross}}$	30.47	MW
W_{net}	30.13	MW
η_{plant}	35.91	%
Heat rate	10,025.16	MJ/MWh
Back work ratio	1.11	%

the condensation pressure increasing the enthalpy drop through the steam turbine and resulting in higher power output and efficiency. The selected absorption chiller has COP of 0.72, a nominal cooling capacity 400 ton with 60.56 kg/s of maximum mass flow rate. The chilled water temperature is 6.67 °C and the chiller electrical consumption is 7.2 kW. Figure 2 shows the proposed system.

2.4.1 Standard operation mode

Under standard mode, the power plant operates according to Fig. 1. The condenser is cooled by the cooling tower water and the absorption chiller cools the water stored in the hot water storage tank. This cold water, after being cooled by the chiller, is stored into the cold water storage tank. When the cold water tank is full, the power plant is ready to operate under repowering mode.

Table 3 Table 3 Fuels studied in this work. Adapted from [21]

Fuel	C	H	S	Other elements	LCV (MJ/kg)	Acid dew point (°C)
Oil 1A	85.20	10.80	0.04	3.96	40.43	101.49
Oil 2B	87.30	11.10	0.74	0.86	41.08	129.03
Oil 1B	85.60	11.30	0.80	2.30	41.16	130.10
Oil 2A	85.30	10.40	2.80	1.50	39.97	142.14

2.4.2 Repowering operation mode

Under repowering mode, the water flow from the cooling tower is bypassed and the cold water from the tank is drained into the condenser and returns to the hot water storage tank. The mass flow rate needed to cool the condenser is considerably greater than the mass flow rate of cold water that the absorption chiller can provide. Therefore, this repowering operation mode only occurs for a short period of time. Note, that a single stratified tank (with a thermocline) could also be used. Since the absorption chiller is just a component of the overall system studied, a black box approach has been used to model this component.

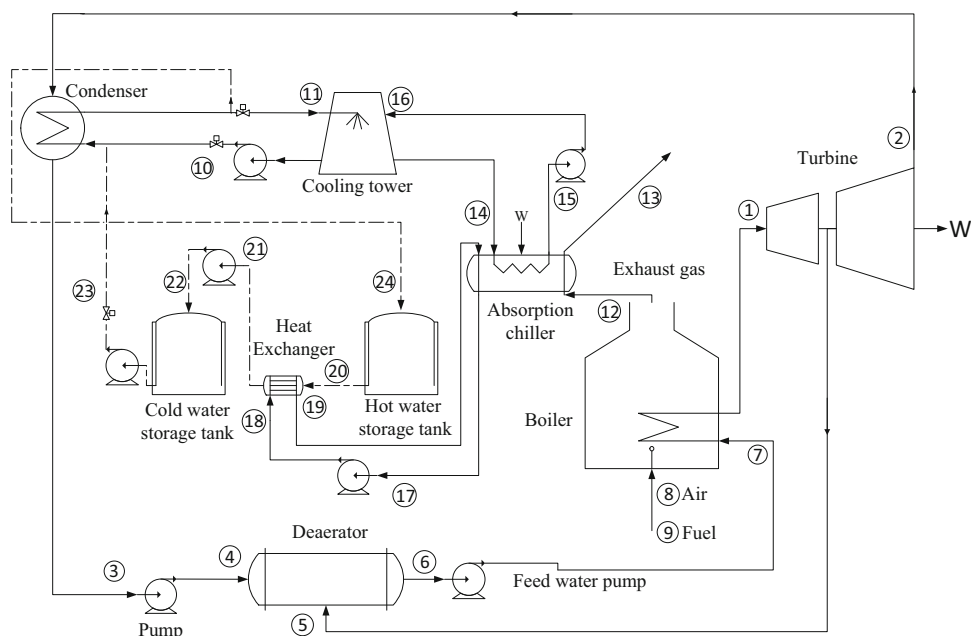
2.4.3 Determination of the repowering operation time

During repowering mode, the cold water is drained into the condenser with mass flow rate \dot{m}_{resf} , while the cold water storage tank receives water cooled by the chiller with mass flow rate \dot{m}_{chiller} . The length of time in which the repowering mode t_R occurs is determined by:

$$M_{\text{water}} = (\dot{m}_{\text{resf}} - \dot{m}_{\text{chiller}})t_R, \quad (1)$$

M_{water} is the tank capacity in mass (kg). After the full discharge of cold water, the cycle returns to operation in standard mode during a period of time t_S .

Fig. 2 Proposed power plant with absorption chiller



$$M_{\text{water}} = \dot{m}_{\text{chiller}} t_S \tag{2}$$

For the proposed system, a tank with a capacity of 2915.29 m³ is required. Considering that the tank diameter is equal to its height both values are 15.48 m. The total power generated during the repowering operation mode is given by:

$$\dot{W}_{\text{repowered}} = \dot{W}_{\text{plant}} - \dot{W}_{\text{chiller}} - \dot{W}_{\text{pump}} \tag{3}$$

\dot{W}_{plant} is the power produced by power plant, \dot{W}_{chiller} is the electrical power consumed by the chiller and \dot{W}_{pump} is the power consumed by cold water pump.

2.4.4 Condenser analysis

During standard operation, the heat rejected by the condenser \dot{Q}_{rej} is determined by Eqs. (4) and (5):

$$\dot{Q}_{\text{rej}} = U_C A_C \Delta T_{\text{ml}} \tag{4}$$

$$\dot{Q}_{\text{rej}} = \dot{m}_w \Delta h_{\text{Cond}} \tag{5}$$

U_C is the overall heat transfer coefficient considered as 2.5 kW/m² K [13]. A_C is the total area of heat exchange. \dot{m}_w is the mass flow rate of working fluid condensing. Δh_{Cond} is the working fluid enthalpy variation in the condenser. ΔT_{ml} is the logarithmic mean temperature difference of the streams in the condenser. The calculated area of heat exchange for the condenser is 2068 m². Figure 3a shows the arrangement for the condenser during standard operation mode.

During repowering operation, the heat rejected by the condenser is calculated iteratively, as indicated at Table 4, by Eqs. (6)–(8). Equation (9) is the objective function that must be zero. \dot{m}_{w_rep} is the working fluid mass flow rate for

the repowering operation mode, C_p is the specific heat of the water and ΔT_{23-20} is the temperature difference between streams 20 and 23 shown in Fig. 3b.

$$\dot{Q}_{\text{rej1}} = U_C A_C \Delta T_{\text{ml}} \tag{6}$$

$$\dot{Q}_{\text{rej2}} = \dot{m}_{w_rep} \Delta h_{\text{Cond}} \tag{7}$$

$$\dot{Q}_{\text{rej3}} = \dot{m}_{\text{resf}} C_p \Delta T_{23-20} \tag{8}$$

$$D_{\text{diff}} = \sqrt{(\dot{Q}_{\text{rej1}} - \dot{Q}_{\text{rej2}})^2 + (\dot{Q}_{\text{rej1}} - \dot{Q}_{\text{rej3}})^2} \tag{9}$$

2.4.5 Results

During repowering operation, the condensation temperature decreases resulting in less heat rejected to the ambient. Therefore, the plant efficiency and power generation are increased. A reduction of 2.24% in the steam quality, x_{steam} , at steam turbine exit is noticed. The lower value of steam quality may increase the maintenance requirements due to the erosion caused by the impact of water droplets on the blades of the turbine low pressure stages. Table 5 shows a comparison between the condenser parameters during standard and repowering operation. Table 6 shows the calculated global data for the power plant in repowering operation mode. Table 7 shows the benefits of the use of the absorption chiller to the studied plant.

2.4.6 System optimization

Different ratios of cooling water from cooling tower and the cold water, cooled by the absorption chiller, were

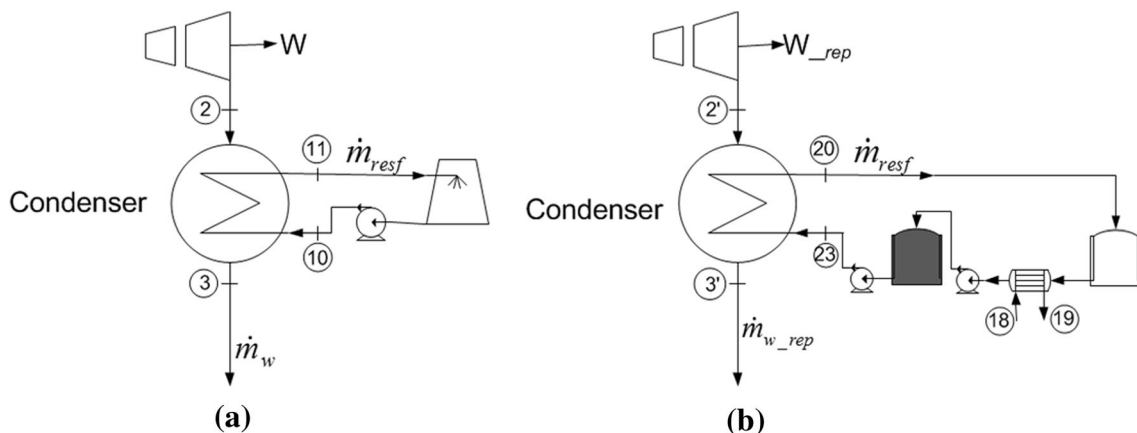


Fig. 3 Arrangement for the condenser: a standard operation mode and b repowering operation mode

Table 4 Parameters used for iterative calculation for the heat rejected by the condenser

Independent variable	Main dependent variables	Lower bound	Upper bound
T_{sat}		20 °C	45 °C
T_{11}		30 °C	40 °C
	T_{10}	15 °C	30 °C
	\dot{m}_{w_rep}	12 kg/s	25 kg/s
	x_{steam}	80%	95%

x_{steam} steam quality at steam turbine exit

Table 5 Condenser parameter comparison

Parameters	Standard mode	Repowering mode	Unit
ΔT_{ml}	9.10	8.75	°C
U_c	2.50	2.50	kW/m ² K [13]
$T_{condensation}$	45.00	26.63	°C
\dot{Q}_{rej}	47,060.40	45,237.17	kW
A_c	2068.00	2068.00	m ²
x_{steam}	83.02	80.78	%

Table 6 Calculated global data during repowering operation

Global data	Value	Unit	
W_{tot_gross}	32.29	MW	
W_{tot_net}	31.94	MW	
η_{cycle}	38.07	%	
Heat rate	9457.18	MJ/MWh	
t_S	83,730.59	s	23.26 h
t_R	2669.41	s	0.74 h
M_{water}	2,915,291.29	kg	

mixed and tested to find the best ratio to increase power generation. A higher temperature mixture enables a longer period of repowering. On the other hand, lower

Table 7 Main results

Main results found	Value	Unit
Net power gain	1.81	MW
Efficiency gain	2.16	%
Decrease in condenser temperature	18.37	°C
Daily time length for repowering mode	44 m:29 s	–

temperatures last for short periods but the increase in power production is more accentuated. Figure 4 shows the daily energy gain according to the percentage of chilled water mixed with cooling tower water. The maximum increment in energy is obtained using 100% of chilled water for a shorter period of time instead of mixed water for a longer period of time. Therefore, the results previously presented correspond to the optimized ratio.

2.5 Second proposal: organic Rankine cycle

In this section, the ORC configurations, thermodynamic model and methodology are described. Both recuperative ORC (RORC) and non-recuperative ORC (NORC) were tested. Supercritical conditions were used for fluids which perform better in these conditions.

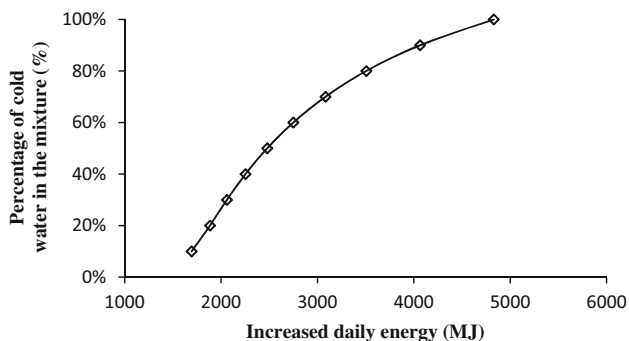


Fig. 4 Energy gain according to the percentage of chilled water in the mixture

2.5.1 Non-recuperative ORC

Figure 5 shows the possible configurations for the NORC in the $T-s$ diagrams. Subcritical conditions are shown in Fig. 5a. The fluid enters the turbine with temperature and pressure defined in state 14. Then it expands to the condensation pressure (state 15) and enters the condenser, leaving at the same pressure but as saturated liquid. This liquid is pumped to the evaporation pressure (state 17), which is lower than the critical

pressure, and enters the economizer, where it is heated at constant pressure to saturated liquid state (state 24). Next, through the evaporator, the fluid evaporates and leaves as saturated vapor (state 25). If it is advantageous for the cycle, the fluid is superheated next, reaching state 14. Otherwise, state 14 is the same as state 25. The heating process from state 17 to state 14 is obtained using the waste heat source (boiler exhausting gases) that goes from state 12 to state 13 as shown in Fig. 5a.

Figure 5b shows the supercritical configuration for the NORC. The difference between both configurations is that the fluid enters the turbine in a supercritical condition. That means that the temperature and pressure of the fluid are above critical values. Therefore, there is no evaporation process; the supercritical fluid goes directly from state 17 to state 14, above saturation line. Fluids that can operate in supercritical condition with the given heat source temperature were tested to confirm if they perform better that way.

2.5.2 Recuperative ORC

This configuration is represented in Fig. 6. The reason to use this layout is because some fluids leave the turbine after

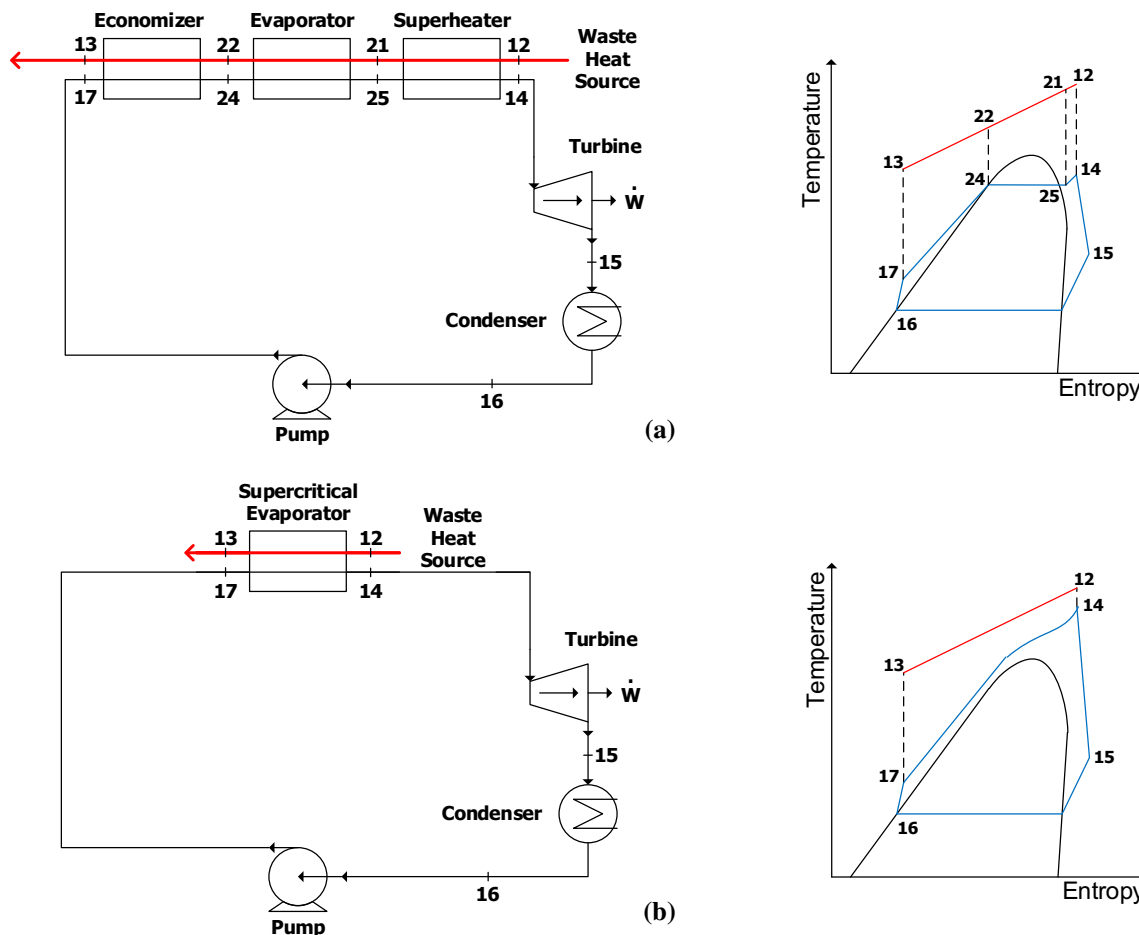


Fig. 5 Configuration and $T-s$ diagram of NORC: a subcritical and b supercritical

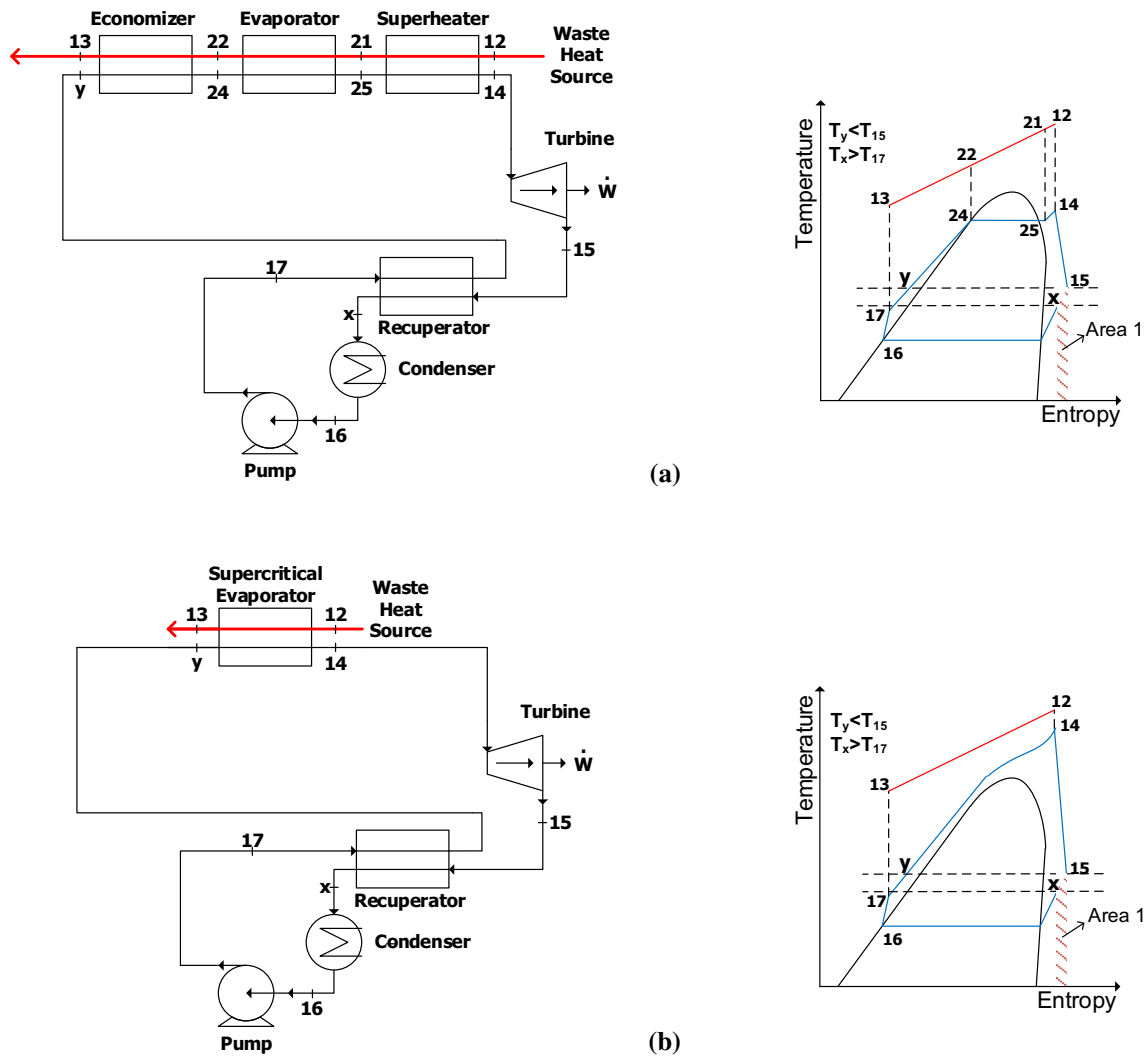


Fig. 6 Configuration and T - s diagram of RORC: a subcritical and b supercritical

expansion as superheated vapor. The use of a recuperator allows transferring heat from the superheated vapor to the fluid leaving the pump. The condition for applying this layout is that $T_{15} > T_{17}$. The fraction of the heat recovered is shown in Fig. 6 as area 1. This heat would originally be lost in condenser to the ambient. Similar to the NORC, the RORC can also be either subcritical (Fig. 6a) or supercritical (Fig. 6b) depending on same factors exposed in Sect. 2.5.1.

2.5.3 Thermodynamic model

To compare the results of the proposals, the heat source characteristics for the ORC are the same used for the absorption chiller. The exhaust gas mass flow rate is 35.73 kg/s at 175.61 °C. The specific heat used was the same used for the absorption chiller (1.087 kJ kg⁻¹ K⁻¹). The minimum temperature at state 13 was limited to 5 °C

above the acid dew point at 106.5 °C. All components were modeled at steady state and the same assumptions from Sect. 2.1 were applied. Table 8 gives the parameters used for the simulations. Some of these parameters were set according to Mazetto et al. [17].

The isentropic efficiencies of the expander and pump are given, respectively, in Eqs. (10) and (11).

$$\eta_{t,ise} = \frac{h_{14} - h_{15}}{h_{14} - h_{15,ise}}, \tag{10}$$

$$\eta_{p,ise} = \frac{h_{17,ise} - h_{16}}{h_{17} - h_{16}}. \tag{11}$$

In these equations h is the specific enthalpy at the subscripted states. The energy balances for the expander and pump are given, respectively, in Eqs. (12) and (13).

$$\dot{W}_t = \dot{m}_{wf}(h_{14} - h_{15}), \tag{12}$$

$$\dot{W}_p = \dot{m}_{wf}(h_{17} - h_{16}), \tag{13}$$

Table 8 ORC specifications for simulation

Parameter	Value	Unit	References
Expander isentropic efficiency ($\eta_{t,ise}$)	80	%	Mazetto et al. [17]
Pump isentropic efficiency ($\eta_{p,ise}$)	75	%	Mazetto et al. [17]
Recuperator effectiveness (ϵ_r)	85	%	Val et al. [27]
Pinch temperature difference at condenser	10	°C	Mazetto et al. [17]
Pinch temperature difference at evaporator	10	°C	Mazetto et al. [17]
Exhaust gas temperature at state 12 (T_{12})	175.61	°C	–
Minimum temperature at state 13 (T_{13})	106.5	°C	–
Exhaust gas mass flow rate (\dot{m}_g)	35.73	kg/s	–
Exhaust gas average specific heat (C_{p_g})	1.087	kJ/kg K	–

\dot{m}_{wf} is the mass flow rate of working fluid. Equations (14)–(17) give the energy balances of the economizer, evaporator, super-heater and supercritical evaporator.

$$\dot{m}_g C_{p_g} (T_{22} - T_{13}) = \dot{m}_{wf} (h_{24} - h_{17}), \tag{14}$$

$$\dot{m}_g C_{p_g} (T_{21} - T_{22}) = \dot{m}_{wf} (h_{25} - h_{24}), \tag{15}$$

$$\dot{m}_g C_{p_g} (T_{12} - T_{21}) = \dot{m}_{wf} (h_{14} - h_{25}), \tag{16}$$

$$\dot{m}_g C_{p_g} (T_{12} - T_{13}) = \dot{m}_{wf} (h_{14} - h_{17}). \tag{17}$$

The recuperator effectiveness is defined in Eq. (18). Energy balance for this equipment is given by Eq. (19)

$$\epsilon_r = \frac{T_{15} - T_x}{T_{15} - T_{17}}, \tag{18}$$

$$h_{15} - h_x = h_y - h_{17}. \tag{19}$$

The heat transferred from the exhaust gases to the working fluid is calculated by Eq. (20). Equations (21) and (22) give the net power generated and cycle efficiency.

$$\dot{Q}_H = \dot{m}_{wf} (h_{14} - h_{17}), \tag{20}$$

$$\dot{W}_{net} = \dot{W}_t - \dot{W}_p, \tag{21}$$

$$\eta_{ORC} = \frac{\dot{W}_{net}}{\dot{Q}_H}. \tag{22}$$

2.5.4 Methodology for optimization of the ORCs

To find the configuration for the highest net power output, 23 fluids were tested. Table 9 shows the fluid candidates and their respective properties. The selected fluids comply with Kyoto and Montreal protocols and are the same used by Mazetto et al. [17]. The software EES® [16] was used for modeling the cycle. This software has a large database of fluid properties and is well known in scientific media. The optimization method employed was the Genetic Algorithm which consists on a computational model inspired by Darwin’s theory of evolution in search for the global optima. At the first moment, the software calculates the objective

Table 9 Working fluid candidate properties

Substance	Type	T_{crit} (°C)	P_{crit} (kPa)
Benzene	Dry	288.9	4894
Isobutane	Dry	134.7	3640
<i>n</i> -Butane	Dry	152.0	3796
<i>n</i> -Decane	Dry	344.6	2103
<i>n</i> -Dodecane	Dry	385.0	1817
<i>n</i> -Heptane	Dry	267.0	2727
<i>n</i> -Hexane	Dry	234.7	3058
<i>n</i> -Nonane	Dry	321.4	2281
<i>n</i> -Octane	Dry	296.2	2497
<i>n</i> -Pentane	Dry	196.5	3364
Isopentane	Dry	187.2	3370
Cyclohexane	Isentropic	280.5	4081
Toluene	Isentropic	318.6	4126
R123	Isentropic	183.7	3668
R134a	Isentropic	101.0	4059
R141b	Isentropic	204.2	4249
R142b	Isentropic	137.1	4055
R245fa	Isentropic	154.0	3651
R502	Wet	82.16	4074
R717	Wet	132.3	11,330
Ethanol	Wet	241.6	6268
Propane	Wet	96.68	4247
Water	Wet	374.0	22,060

function for a population of random values for the variables. After that, a new generation is chosen taking into account the best previous results and new results are calculated. After some generations, it is possible to find the optimal values for these variables. To avoid local maxima, the method also applies mutations in each generation, which are values far from the population tested, to find the global maximum.

To maximize the objective function (net power output, \dot{W}_{net}) given by Eq. (21), the optimized variables were T_{14} and P_{14} , respecting the constraint parameters from Table 8: pinch temperature difference at evaporator and minimum

Table 10 Optimized properties for non-recuperative ORC

Substance	\dot{m}_{wf} (kg/s)	P_{14} (kPa)	T_{14} (°C)	Condition
R502	14.24	4074	165.6	Supercritical
R717	2.623	13,644	165.6	Supercritical
Ethanol	2.495	287	164.2	Subcritical
Propane	6.46	7959	165.6	Supercritical
Water	1.03	111.1	165.6	Subcritical

temperature at state 13 (T_{13}). For the subcritical ORCs, the maximum turbine inlet temperatures and pressures allowed were set to be the critical temperatures and pressures of each fluid tested. For the supercritical states, the critical temperatures and pressures were set as the minimum turbine inlet temperatures and pressures, respectively.

2.5.5 Results

The best performance fluids for non-recuperative ORC are presented in Table 10. The best performance fluids for recuperative ORC are presented in Table 11. Both tables present, for each substance, the optimized values for the turbine inlet temperature (T_{14}) and pressure (P_{14}), as well as the corresponding value for the mass flow rate (\dot{m}_{wf}). It also indicated the condition of the fluid at this state, which can be subcritical or supercritical.

The turbine inlet temperature and pressure vary significantly depending on the chosen working fluid. Some fluids, such as *n*-dodecane enter the turbine with an absolute pressure of 3.65 kPa, which is much lower than the atmospheric pressure. On the other hand, the highest pressure is required by the R717 (13.6 MPa). The mass flow rate also varies widely, from 1.03 kg/s for water to 13.24 kg/s for R502. Most substances with critical temperature lower than the waste heat source temperature reached supercritical condition. This is due to the better matching between the heat source temperature curve and working fluid temperature curve [14]. These results can be better observed in Fig. 7.

As an overall result, *n*-butane presented the best results with a net power output of 409.3 kW and a cycle efficiency of 15.25%. Following this, R245fa comes with 408.5 kW of net power output and 15.22% of efficiency. Both reached supercritical condition. The poorest results were from R502 with a power output of 102.9 kW and 3.83% efficiency. Carnot efficiency is used to evaluate how far the ORC is from thermodynamic upper limit. The Carnot efficiency η_{Carnot} is defined in Eq. (23).

$$\eta_{Carnot} = 1 - \frac{T_L}{T_H}, \quad (23)$$

T_L is the condensation temperature, the lowest temperature of the cycle. T_H is the temperature in which the heat is

Table 11 Optimized properties for recuperative ORC

Substance	\dot{m}_{wf} (kg/s)	P_{14} (kPa)	T_{14} (°C)	Condition
Benzene	5.566	236.7	120.6	Subcritical
Isobutane	7.165	4025	165.6	Supercritical
<i>n</i> -Butane	6.495	3796	165.6	Supercritical
<i>n</i> -Decane	6.576	15.42	112.9	Subcritical
<i>n</i> -Dodecane	6.519	3.646	113	Subcritical
<i>n</i> -Heptane	6.409	156.2	117.8	Subcritical
<i>n</i> -Hexane	6.294	369.3	118.3	Subcritical
<i>n</i> -Nonane	6.157	36.5	116.9	Subcritical
<i>n</i> -Octane	6.481	71.2	114.8	Subcritical
<i>n</i> -Pentane	6.614	879.1	119.8	Subcritical
Isopentane	6.876	1108	123.5	Subcritical
Cyclohexane	5.785	259.2	118.2	Subcritical
Toluene	5.798	98.2	119.8	Subcritical
R123	14.07	1063	132.7	Subcritical
R134a	14.12	6256	165.6	Supercritical
R141b	10.82	987.8	119.8	Subcritical
R142b	11.94	4109	165.6	Supercritical
R245fa	12.48	3651	165.6	Supercritical

transferred to the cycle. The mean thermodynamic temperature of the exhaust gases is defined in Eq. (24).

$$T_{mean} = \frac{\Delta h}{\Delta s}, \quad (24)$$

Δh is the enthalpy drop and Δs is the entropy variation of flow. $T_{mean} = 140.9$ °C for the ORC optimized with *n*-butane as working fluid and $T_L = 50$ °C (temperature at condenser). Considering $T_H = T_{mean}$, the corresponding Carnot efficiency is 21.95%. Therefore, the ORC with best results has an efficiency relative to Carnot (η_{ORC}/η_{Carnot}) of 69.48%, which is a notorious result.

2.5.6 Comparison between ORC-assisted and chiller-assisted power plants

To compare the results from both proposals, it was necessary to equalize the time periods. The use of an absorption chiller resulted in a gain of 1.81 MW for a period of 2669.41 s. On a daily basis, the result is equivalent to an average gain of 55.92 kW which represents an increase of 0.06% in the efficiency of the studied plant. The comparison results can be seen in Table 12.

3 Conclusion

The objective of this work was to compare two possible proposals to increase the power generated by an already existing conventional Rankine cycle-based power plant.

Fig. 7 Optimization results

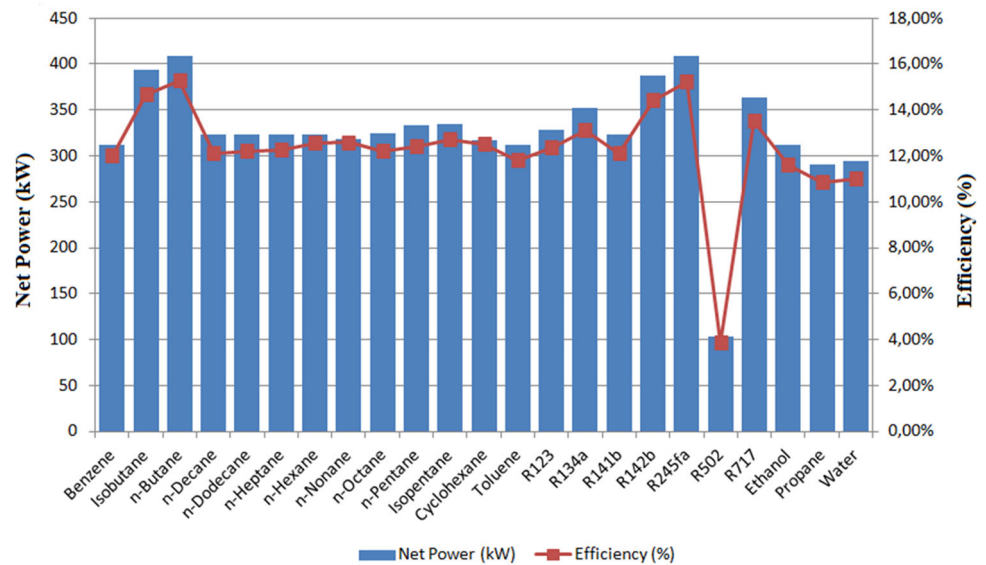


Table 12 Comparison between ORC-assisted and chiller-assisted power plants

Results	Abs. chiller	ORC (<i>n</i> -butane)
Net power gain (kW)	55.92	409.3
Efficiency increase (%)	0.07	0.42

The two systems tested were an absorption chiller to reduce the temperature of condenser cooling water and an organic Rankine cycle, both powered by the recoverable (above dew point) waste heat from the boiler exhaust gases. ORC optimizations were conducted using 23 different fluids searching for the optimal expander inlet temperature and pressure to obtain the maximum net power generation.

For the specific conditions evaluated, the absorption chiller increased the power output in 1.81 MW for a period of 44 min and 29 s, which represents a daily average gain of 55.92 kW. The Recuperative ORC with *n*-butane represented a gain of 409.3 kW in net power generation under the optimized conditions. These results indicate that, from a thermodynamic point of view, it is more advantageous to use an ORC coupled to the Rankine cycle-based power plant studied than an absorption chiller. Further studies need to be conducted to compare the economical benefits of both systems. Other technologies may also be applied to use the energy from the exhaust gases. Boiler design improvements such as addition of extra economizer or air pre-heaters are interesting options. These improvements, however, will change the temperature profile of the boiler, therefore, the evaluation of operational feasibility and changes in control system of this equipment will be required.

Acknowledgements Vitor R. Seifert and Yuri M. Barbosa gratefully acknowledge the Industrial Engineering Program, Federal University

of Bahia. These authors also acknowledge FAPESB (Fundação de Amparo ao Pesquisador do Estado da Bahia) for the provision of master scholarships. Ednildo A. Torres would like to thank the National Council for Scientific and Technological Development (CNPq).

References

1. ANP (2011) Agência Nacional de Petróleo, Gás Natural e Biocombustíveis. RESOLUÇÃO ANP N° 65. <http://www.anp.gov.br/wwwanp/?dw=63899>. Accessed 03 June 2017
2. Agnew B, Alaktiwi A, Anderson A, Potts I (2004) Simulation of a combined Rankine–absorption cycle. *J Appl Therm Eng* 24:1501–1511
3. Battista D, Mauriello M, Cipollone R (2015) Waste heat recovery for an ORC-based power unit in a turbocharged diesel engine propelling a light duty vehicle. *Appl Energy* 152:109–120
4. Calise F, D’accadia M, Vicidomini M, Scarpellino M (2015) Design and simulation of a prototype of a small-scale solar CHP system based on evacuated flat-plate solar collectors and organic Rankine cycle. *Energy Convers Manag* 90:347–363
5. Camporeale S, Pantaleo A, Ciliberti P, Fortunato B (2015) Cycle configuration analysis and techno-economic sensitivity of biomass externally fired gas turbine with bottoming ORC. *Energy Convers Manag* 105:1239–1250
6. Celis C, Avellar VP, Ferreira SB, Braga, SL (2007) Evaluation of different alternatives of power augmentation for an existing combined cycle power plant in Brazil. *J Power ASME Turbo Expo 2007: Power for Land, Sea, and Air* 3:603–612. doi:10.1115/GT2007-27172
7. Chacartegui R, Sánchez D, Muñoz J, Sánchez T (2009) Alternative ORC bottoming cycles for combined cycle power plants. *Appl Energy* 86:2162–2170
8. Chacartegui R, Becerra J, Blanco M, Muñoz-Escalona J (2015) A humid air turbine—organic Rankine cycle combined cycle for distributed microgeneration. *Energy Convers Manag* 104:115–126
9. Clemente S, Micheli D, Reini M, Taccani R (2013) Bottoming organic Rankine cycle for a small scale gas turbine: a comparison of different solutions. *Appl Energy* 106:355–364

10. Demierre J, Henchoz S, Favrat D (2012) Prototype of a thermally driven heat pump based on integrated organic Rankine cycles (ORC). *Energy* 41:10–17
11. Galindo J, Ruiz S, Dolz V, Royo-Pascual L, Haller R, Nicolas B, Glavatskaya Y (2015) Experimental and thermodynamic analysis of a bottoming organic Rankine cycle (ORC) of gasoline engine using swash-plate expander. *Energy Convers Manag* 103:519–532
12. Ganapathy V (1994) *Steam plant calculations manual*, 2nd edn, rev. and expanded. ABCO Industries, Abilene
13. Kakaç S, Liu H (2002) *Heat exchangers. Selection, rating and thermal design*. CRC Press, New York
14. Kalra C, Becquin G, Jackson J, Laursen AL, Chen H, Myers K, Klockow H, Zia J (2012) High-potential working fluids and cycle concepts for next-generation binary organic Rankine cycle for enhanced geothermal systems. In: *Thirty-seventh workshop on geothermal reservoir engineering*, Stanford, USA
15. Kim TS, Ro ST (2000) Power augmentation of combined cycle power plants using cold energy of liquefied natural gas. *J Energy* 25:841–856
16. Klein SA (2015) *Engineering equation solver (EES)*, Academic Professional V9.901
17. Mazetto B, Silva J, Oliveira S Jr (2015) Are ORCs a good option for waste heat recovery in a petroleum refinery? *Int J Thermodyn* 18:161–169
18. Muñoz J, Martínez-Val JM, Abbas R, Abánades A (2012) Dry cooling with night cool storage to enhance solar power plants performance in extreme conditions areas. *J Appl Energy* 92:429–436
19. Portal Brasil (2011) ANP aprova abastecimento com Diesel de baixo teor de enxofre a partir de janeiro de 2012. <http://www.brasil.gov.br/infraestrutura/2011/12/anp-aprova-abastecimento-com-diesel-de-baixo-teor-de-enxofre-a-partir-de-janeiro-de-2012>. Accessed 03 June 2017
20. Rahbar K, Mahmoud S, Al-Dadah R, Moazami N (2015) Modeling and optimization of organic Rankine cycle based on a small-scale radial inflow turbine. *Energy Convers Manag* 91:186–198
21. Resolução ANP N° 3 DE 27/01/2016. <https://www.legisweb.com.br/legislacao/?id=315822>. Accessed 05 June 2017
22. Shirazi A, Najafi B, Aminyavari M, Rinaldi F, Taylor RA (2014) Thermal–economic–environmental analysis and multi-objective optimization of an ice thermal energy storage system for gas turbine cycle inlet air cooling. *Energy* 69:212–226
23. Shu G, Gao Y, Tian H, Wei H, Liang X (2014) Study of mixtures based on hydrocarbons used in ORC (organic Rankine cycle) for engine waste heat recovery. *Energy* 74:428–438
24. Silva JAM, Pinto CP, Rucker C, Oliveira S Jr (2011) Exergy and thermoeconomic evaluation of a refinery utilities plant. In: *Proceedings of ECOS 2011—24th international conference on efficiency, cost, optimization, simulation and environmental impact of energy systems*, Novi Sad, Serbia
25. Silva JAM (2013) *Desempenho Exergo-Ambiental do Processamento de Petróleo e seus Derivados* (in portuguese). PhD thesis, Mechanical Engineering Department of University of São Paulo
26. Song J, Song Y, Gu C (2015) Thermodynamic analysis and performance optimization of an organic Rankine cycle (ORC) for engine waste heat recovery. *Energy* 82:976–985
27. Val C, Silva J, Junior S (2016) Deep water cooled ORC for floating oil platform applications. In: *ECOS 2016—the 29th international conference on efficiency, cost, optimization, simulation and environmental impact of energy systems*, Slovenia